INVESTIGATION OF METASTATIC POTENTIAL OF BREAST CANCER CELLS IN LUNG-ON-A-CHIP

A Thesis Submitted to
the Graduate School of Engineering and Sciences of
Izmir Institute of Technology
in Partial Fulfillment of the Requirements for the Degree of

MASTER OF SCIENCE

in Molecular Biology and Genetics

by
Deniz Cemre TURGUT

July 2023
İZMİR

We approve the thesis of **Deniz Cemre TURGUT**

Examining Committee

Prof. Dr. Devrim PESEN OKVUR
Molecular Biology and Genetics, Izmir Institute of Technology

Prof. Dr. Özden YALÇIN ÖZUYSAL
Molecular Biology and Genetics, Izmir Institute of Technology

Assoc. Prof. Dr. Yavuz OKTAY
Basic and Translational Research Program, Izmir Biomedicine and Genome Centre

19 July 2023

Prof. Dr. Devrim PESEN OKVUR
Supervisor, Molecular Biology and Genetics
Izmir Institute of Technology

Prof. Dr. Özden YALÇIN ÖZUYSAL
Head of the Department of Molecular Biology and Genetics

Prof. Dr. Mehtap EANES
Dean of the Graduate School of Engineering and Science

ACKNOWLEDGEMENT

First, I would like to thank my jury members, Prof. Devrim Pesen Okvur, Prof. Özden Yalçın Özuysal and Assis. Prof. Yavuz Oktay for the time and expertise each of you shared during the evaluation process. In addition, I am thankful for Prof. Volkan Seyrantepe and Seçil Akyıldız Demir, PhD for supplying mice cadavers to make this research possible.

I would like to extend my gratitude for Prof. Devrim Pesen Okvur since she has consistently encouraged and challenged me to push the boundaries of my capabilities, fostering personal and intellectual growth. During this study, I have also felt lucky to have Prof. Özden Yalçın Özuysal as an informal co-supervisor. They have led us by example and set the highest standards for academic excellence and professionalism. Their mentorship has not only improved the quality of my work, but they have been a listening ear during moments of doubt.

I cannot express how I feel truly fortunate to study with my thesis mate, Perge Bilgesu Tosunoğlu. It has been an honour and joy to work with you side by side. I believe our strong friendship has been the most important result of this study. I look forward to our everlasting collaboration in life and friendship.

I would like to express my appreciation to the members of Controlled *in vitro* Microenvironment Lab (2021-2023) for being collaborative and supportive. I also would like to thank Ata Merdan, my stagier, for helping me in experiments without an excuse. His presence is always treasured. I shall extend my heartfelt gratitude to Aslı Kısım, PhD for her valuable bits of advice and discussions for our experiments.

As for my family, your love and support have been my foundation, and I am forever grateful for your role in my academic and personal growth. My beloved cat Lulu and dog Parfait have been a constant source of serotonin. Dad, your presence, and encouragement have been the cornerstone of my personal and scholarly achievements.

At last, I would like to thank my chosen family of friends, Mehmet, Melis, Onur and Feyza, who have been a source of laughter, peace, and encouragement throughout my academic journey. Thank you all for letting me be me. I am profoundly grateful for Melis as being my partner in Izmir Institute of Technology and as my best friend in life. You have always been by my side quite literally and I know you will always be.

ABSTRACT

INVESTIGATION OF METASTATIC POTENTIAL OF BREAST CANCER CELLS IN LUNG-ON-A-CHIP

Breast cancer stands as the most prevalent cancer among women and ranks as the second leading cause of cancer-related fatalities globally. The primary contributor to mortality is metastasis. Triple negative breast cancer exhibits a tendency to metastasize to the lungs, as lungs identified as one of the most common targets of breast cancer metastases. However, to study the precise mechanisms governing this organ-specific metastatic pattern requires a sophisticated 3D lung model, which can truly recapitulate lung physiology and architecture. This study explores the metastatic behaviour of MDA-MB-231 breast cancer cells and their interaction with tumour-associated macrophages (TAMs) within a 3D lung model created through a novel biopsy punch technique. The obtained punched lung tissues are integrated into microphysiological systems presenting a hybrid 3D culture model for lung studies. The key findings of this research reveal the effectiveness of biopsy punches in preserving tissue integrity and ensuring a consistent size distribution. Additionally, the study demonstrates the viability of lung tissues for up to 72 hours. Most notably, MDA-MB-231 cells exhibit a significant capacity to invade the punched lung tissues with even greater infiltration observed in the presence of differentiated U-937 cells. These findings provide valuable insights into the metastatic potential of breast cancer cells and highlight the importance of TAMs in facilitating cancer progression within a 3D lung microenvironment. This novel tissue culture technique opens new avenues for studying cancer metastasis, precision medicine and tumour-microenvironment interactions.

ÖZET

MEME KANSERİ HÜCRELERİNİN METASTATİK POTANSİYELİNİN ÇİP-ÜZERİ-AKCİĞER KULLANILARAK ARAŞTIRILMASI

Meme kanseri kadınlar arasında en sık görülen kanser olup, dünya çapında kansere bağlı ölümlerin önde gelen ikinci nedenidir. Mortaliteye katkıda bulunan birincil faktör ise metastazdır. Üçlü negatif meme kanseri, akciğerlere metastaz yapma eğilimi gösterir. Bununla birlikte akciğerler, meme kanseri metastazlarının en yaygın hedeflerinden biri olarak tanımlanır. Bu yüzden, akciğere özgü metastatik hareketi yöneten kesin mekanizmaları incelemek, akciğer fizyolojisini ve yapısını gerçekten karşılayabilen bir 3 boyutlu akciğer modelini gerektirir. Bu çalışma, MDA-MB-231 meme kanseri hücrelerinin metastatik davranışını ve bunların, yeni bir biyopsi delme tekniği ile oluşturulan 3 boyutlu akciğer modeli içerisinde tümörle ilişkili makrofajların (TAM'ler) etkisini araştırmaktadır. Elde edilen delinmiş akciğer dokuları, akciğer çalışmaları için hibrit bir 3 boyutlu kültür modeli sunan mikrofizyolojik sistemlere entegre edilir. Bu araştırmanın temel bulguları, biyopsi yumruklarının doku bütünlüğünü koruma ve tutarlı bir boyut dağılımı sağlama konusundaki etkinliğini ortaya koymaktadır. Ayrıca çalışma, biyopsi uygulanmış akciğer dokularının 72 saate kadar canlılığını koruyabildiğini de ortaya koymaktadır. En önemlisi, MDA-MB-231 hücreleri, farklılaşmış U-937 hücrelerinin varlığında gözlenen daha da büyük bir göçle delinmiş akciğer dokularını istila etme konusunda önemli bir kapasite sergiler. Bu bulgular, meme kanseri hücrelerinin metastatik potansiyeli hakkında değerli bilgiler sağlar ve TAM'lerin, 3 boyutlu akciğer mikro ortamında kanser ilerlemesine olan yardımcı rolünün önemini vurgular. Bu yeni doku kültürü tekniği, kanser metastazı, hassas tıp ve tümör-mikroçevre etkileşimlerini incelemek için yeni bir araştırma tekniği ortaya koymaktadır.

To my father…

TABLE OF CONTENTS

LIST OF FIGURES

LIST OF TABLES

CHAPTER 1

INTRODUCTION

1.1. 3D cell culture models

Physiological and tissue-specific pathophysiology research is predominantly based on *in vitro* studies using two-dimensional (2D) cell cultures and *in vivo* studies in relevant animal models. Cells grown as a flat monolayer on an artificial surface is initially used to understand basic principles, which is proceeded with the animal experiments to overcome limitations of 2D cell culture models. Although traditional methods have advantages, they fail to accurately model tissues, predict human response and disease progression. With low success and slow rates in translation of preclinical studies to clinical trials, there is an emerging need of three-dimensional (3D) models, which focuses on mimicking *in vivo* human physiology with a native context (Caleb & Yong 2020). Main key advantages of 3D cultures over traditional methods are the followings.

Compared to 2D cultures, 3D cell culture models are considered more advanced for many reasons. Most significantly, integration of the extracellular matrix in 3D models enables mimicking tissue architecture to study complex cell-matrix and cell-cell interactions. These interactions affect cellular signalling pathways, behaviour, and differentiation. It also preserves original cellular physiology and characteristics. In addition, disease modelling, progression and pathophysiology studies are better suited to observe the cellular and tissue-level changes associated with these conditions. Drug and toxicity assessment is also less relevant in 2D models compare to 3D counterparts due to molecular concentration gradient difference in 3D environment. Moreover, 3D cell culture systems can be manipulated easily to study mechanobiological cues since these systems may include various *in vivo* factors such as matrix stiffness, flow rate and shear stress. Despite outstanding advantages of 3D models, they can be technically challenging to establish and maintain than basic 2D cell culture methods (Habanjar et al, 2021; Vanderburg et al, 2017; Alzeeb et al, 2020).

In addition, 3D models have great potential to replace and reduce animal experiments because animal models lack human relevance, they may fail to replicate complex human physiology. Furthermore, the use of animals in experiments generally holds researchers

responsible for ethical concerns and specific regulations. Maintenance and breeding of animals is more expensive and time consuming. Despite their extensive use, animal experiments are not suitable for high-throughput studies and the environment is not controlled. At last, with increasing awareness among researchers, 3D models are most promising to improve the accuracy of preclinical studies while avoiding animal abuse and cruelty in massive animal experimentation (Hoarau-Véchot et al, 2018).

General advantages of 3D models over traditional methods in cancer research are summarized in Table 1.1. While there are noteworthy reasons to use advanced 3D cell culture models, it is important to recognize that they are not the perfect replacement. The choice of model should be based on specific needs of the research subject. Consequently, a combination of different approaches is the most comprehensive way to accurately model human physiology and disease conditions.

Table 1.1. Advantages of 3D models. (Source: Alzeeb et al, 2020).

System Features	**2D Cell Culture**	**3D Cell Culture**	**Animal Models**
Human relevance	Limited	Better than 2D cell culture	Most physiological environment but human relevance is controversial
Model complexity	Limited	Complex	Most complex
Expression	Stable at early passages	Close to in vivo tumour samples	Close to in vivo tumour samples
Immune system	No but co-culture is possible	No but co-culture is possible	Different in models
Drug screening	Yes	Yes	No
Disease modelling	Naïve	Feasible	Sophisticated
Controlled microenvironment	Yes	Yes	No
Reproducibility	Favourable	Okay	Unsuited
Cost	Low	May require expensive equipment	High
Ethics and regulation	No	No	Differs depending on research

1.2. Lung Physiology and Structure

Lungs are one of the vital organs that are responsible for gas exchange between air and our bloodstream. Air enters the pulmonary system and travels through trachea, which bifurcates into the main bronchi of two lungs, right and left. Further division of bronchi and bronchioles eventually terminates at the alveolar sacs. Here, oxygen diffuses to the bloodstream across the air-liquid interface between alveolar epithelial and endothelial cells. Carbon dioxide, on the hand, is expelled during exhalation. During respiratory cycle, these respiratory organs are intricately designed for efficient respiration, which is directly linked to cellular physiology and organ structure. Proper functioning in diverse range of different cells is crucial to maintain respiratory system and immune defence (Figure 1.1). Including alveolar epithelial cells, fibroblasts, macrophages, endothelial and muscle cells, native lung environment consists of more than 50 different cells that contribute to native extracellular matrix and organotypic mechanobiology (Scheider et al, 2021)

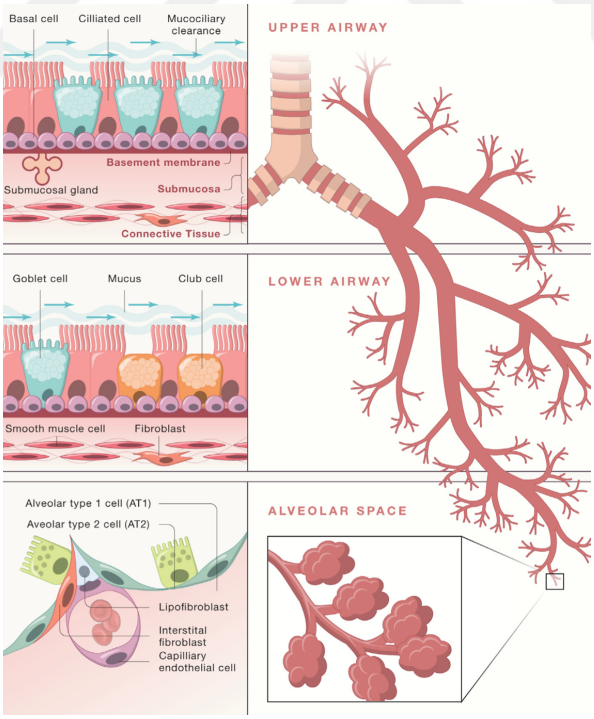

Figure 1.1. Lung physiology and structure. (Source: Scheider et al, 2021).

1.3. 3D Lung Models

3D models are valuable tools to study disease state and progression. As lungs being dynamic organs, incorporating full complexity of these organs are challenging in lung models. Currently, there are various available 3D lung models to investigate the underlaying factors, mechanism of metastasis, pulmonary infections, and test potential therapeutics (Figure 1.2). Spheroid and organoid models are generally used to investigate the lung microenvironment components. Lung microphysiological systems are promising to recreate fluid flow in lung-related physiological environment whereas 3D bioprinted models enables creation of complex 3D matrices. There are also air-liquid interface cultures, which focuses on the terminal functional unit of lungs. In current models, cell lines and primary airway epithelial cells are available to mimic lung physiology. While these approaches have significantly contributed to realistic modelling of lung, researchers still actively address missing points to generate improved models (Shah et al, 2023).

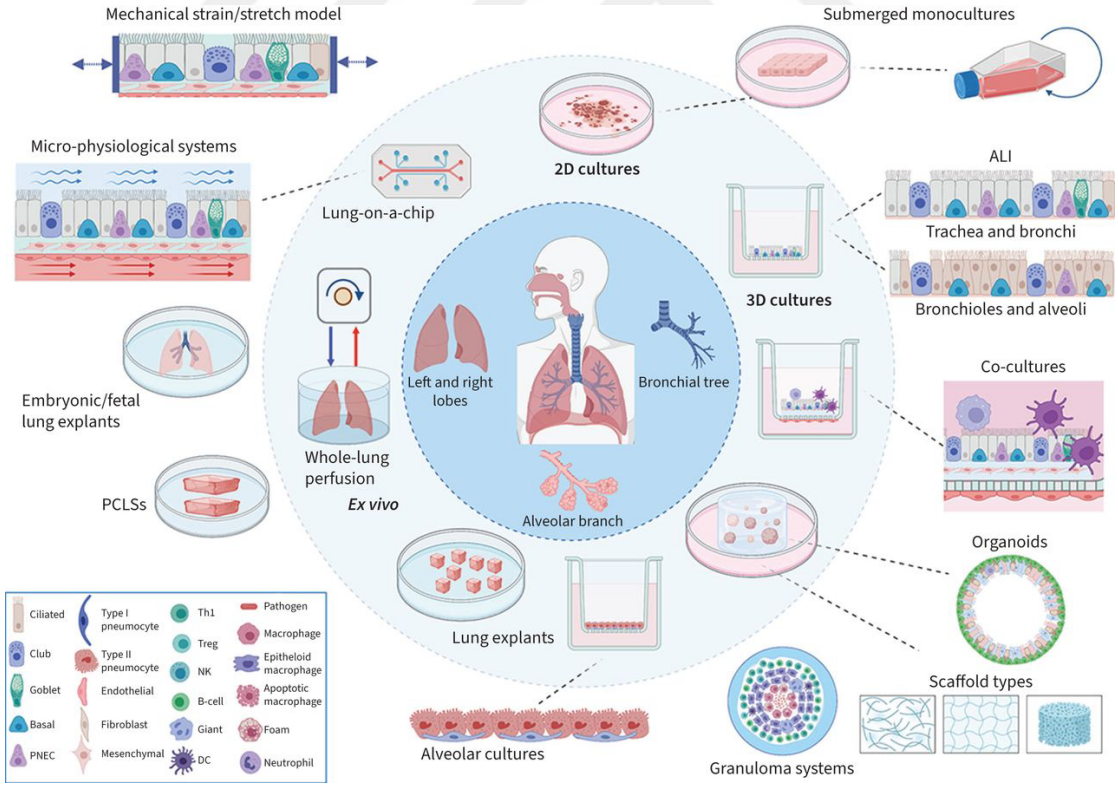

Figure 1.2. *In vitro* and *ex vivo* human lung models. (Source: Humbert et al, 2022).

In addition to *in vitro* 3D lung models, precision-cut lung slices (PCLS) are special *ex vivo* experimental models to study intact tissue pieces. To generate PCLS, removed lung tissues are sectioned into a few millimetres of slices using special equipment such as microtomes or vibratomes. Obtained lung slices are maintained in culture conditions, which mimics natural physiological conditions. The main advantage of using PCLS is that they retain the native architecture and cellular environment of lungs. This allows researchers to bridge the gap between *in vitro* and *in vivo* studies as well as overcome the disadvantages of animal models. Although they are valuable tools for advancing pulmonary health and disease research, preparation of PCLS requires sophisticated instruments, which are not easily accessible.

1.4. Breast Cancer Metastasis to Lung

Breast cancer is one of the most common malignancies worldwide with 2.3 million new cases each year (NAACCR, 2019). Metastatic breast cancer is a leading cause of cancer-related mortalities among women. Metastasis occurs when tumour cells spread from the primary tumour site and to other parts of body. It is a significant factor in the disease progression. Of deaths, 90% of the cases are associated with metastatic complications (Medeiros & Allan, 2019).

As one of the most common sites of metastatic breast cancer, patients with lung-related metastases have 60-70% mortality rate (Wu et al, 2017). Thus, it is important to model and study metastasis of breast cancer cells to lung. Breast cancer can be categorized into various molecular subtypes based on gene expression profiles. These subtypes display specific preferences for particular organs in the metastatic process. For instance, triple negative breast cancer exhibits a tendency to metastasize to the lungs. However, the precise mechanisms governing this organ-specific metastatic pattern remain to be fully understood (Yousefi et al, 2018). To our knowledge, there is only one research that investigates breast cancer metastasis to lung. Fıratlıgil-Yıldırır & Batı-Ayaz et al (2021) studied the metastatic potential of MDA-MB-231 cells, which represent triple negative breast cancer molecular subtype, towards lung microenvironment modelled by lung fibroblasts, WI-38 cells, using organ-on-chips. Their findings have shown that MDA-MB-231 cells are prone to migrate towards lung microenvironment. Hence, a model that

can integrate lung epithelial cells along with native microenvironment is critical to study breast cancer metastasis to investigate lung-related metastasis.

1.5. Tumour-Associated Macrophages in Breast Cancer

In the last decade, studies have shown that cancer is not a merely genetic disorder but rather a complex ecosystem involving highly organized tumour microenvironment (Figure 1.3). A diverse array of non-cancerous cells and their cues are now recognized as pivotal factors to drive cancer pathogenesis. The contribution and state of their effect may change depending on different factors such as inherent characteristics of primary tumour cells, organotypic environment and tumorous stage. Consequently, non-cancerous cells can act to promote or inhibit cancer progression (De Visser & Joyce, 2023).

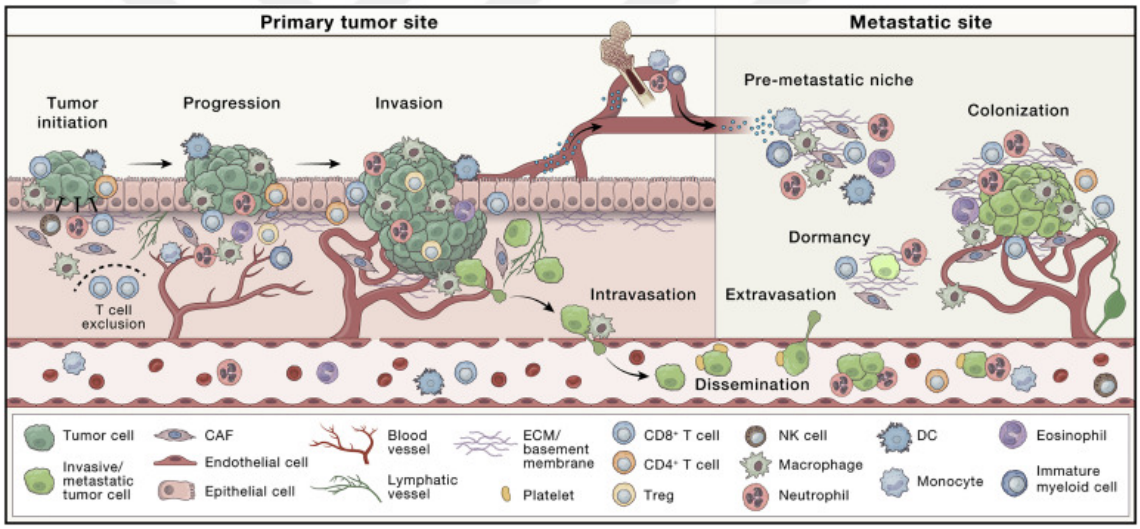

Figure 1.3. Illustration of the complex array in tumour microenvironment. (Source: De Visser & Joyce, 2023).

Among numerous non-cancerous cells, macrophages play significant role at the tumour microenvironment. In breast tumours, macrophages could make up to 50% of tumour mass (Pan et al, 2020). A subpopulation of macrophages called tumour-associated macrophages (TAMs) could aid migration of breast cancer cells into blood vessels, which correlated with metastatic cascade. It has been shown that cancer cells manipulate macrophages with soluble factors to promote tumour growth, invasion, metastasis, and drug resistance. One of which, CSF-1 and EGF paracrine loop enables tumour cells to

migrate alongside macrophages towards blood vessels (Knutsdottir et al, 2016). Clinical data shows that presence of TAMs also correlates with poor prognosis in breast cancer patients (Pan et al, 2020).

Because of their significant interaction, modelling breast cancer cells and TAMs to study cancer cell invasion is critical. U-937 cell lineage is widely utilized as monocytic cells in oncoimmunological research. They are commonly treated with phorbol 12-myristate 13-acetate (PMA) to induce macrophage differentiation. The molecular changes after PMA treatment are studied elsewhere. In a related note, macrophage differentiation increases matrix remodelling protein expression such as metalloproteinases (Nascimento et al, 2022). This suggests that tumour cells could exploit macrophages to redefine existing tumour microenvironment. Knutsdottir et al (2016) showed that the number of both invasive tumour cells and macrophages amplifies the paracrine signalling between cells eventually affecting the migration potential breast cancers. They suggested that modelling 3:1 tumour cell/macrophage ratio, which is also commonly observed in clinical data, is a key parameter to study tumour cell invasion. Therefore, in this study, 3:1 ratio is applied in invasion and infiltration assays.

CHAPTER 2

AIM OF THE RESEARCH

Despite the challenges and limitations, 3D lung models present notable benefits compared to conventional methods. With technological advancement and ongoing efforts by researchers to tackle these limitations, 3D lung models have the potential to offer a more precise mimicking of human lung physiology and structure. Metastatic breast cancer, linked to a reduced survival rate, stands as a significant contributor to global cancer-related fatalities. As the lungs frequently is the destination for metastatic breast cancer cells, a well-established 3D lung model consequently offers an exceptional platform for investigation of breast cancer metastasis to the lungs.

The aim of this research is to investigate the metastatic potential of breast cancer cells within a lung-on-a-chip microenvironment. To achieve this goal, a novel hybrid tissue culture technique that effectively conserves lung physiology and architecture within the lung microphysiological system is aimed to develop. Along with this technique, it is aimed to determine the optimal culture conditions necessary to maximize lung viability after processing This innovative method is the foundation for creating a biologically relevant and dynamic lung microenvironment for the metastasis study. Developed lung microphysiological system is used to simulate the complex interplay between breast cancer cells and the lung. This system enables the investigation breast cancer metastasis to the lung in a controlled and biologically relevant environment. In addition to studying the metastatic potential of breast cancer cells, the system is used to investigate the role of macrophage-like cells within the lung microphysiological system. Therefore, this investigation shows the impact of these immune cells on breast cancer metastasis to the lung, providing critical insights into role of the tumour microenvironment on metastatic processes. By addressing these specific aims, our research will advance our understanding of breast cancer metastasis and contribute to the development of more effective therapeutic strategies.

CHAPTER 3

MATERIAL AND METHODS

3.1. Fabrication of microphysiological system

The microphysiological system (MPS) of this study is composed of three utilisable areas namely A1, A2 and A2 (Figure 3.1). All areas are interconnected. MPS is fabricated by soft lithography. Polydimethylsiloxane (PDMS) is prepared by 1:10 ratio of curing agent: elastomer base (SYLGARDTM 184 Silicone Elastomer Kit). PDMS mixture is vacuumed to avoid any bubbles before casting into the 3D printed moulds. PDMS is polymerized at 37°C for 24 hours and at 60°C for 3 hours. Polymerized MPS is removed from the mould and is cleaned with ultra-pure H_2O, 70% ethanol and ultra-pure H_2O in sequence. MPS is UV-sterilized for 30 minutes, immediately before use.

Figure 3.1. Illustration of microphysiological system which are made of PDMS and have three areas, A1, A2, and A3. The system is interconnected from A1to A2 and A2 to A3.

3.2. Mouse dissection

C57 background wild type mice are cared and mated in Laboratory Animal Production, Care, Application and Research Centre of Izmir Institute of Technology according to Turkish Council on Animal Care (TCAC) regulations. Regardless of sex, 8

to 15 weeks old are euthanized by cervical dislocation by the technicians of Laboratory Animal Production, Care, Application and Research Centre of Izmir Institute of Technology. Mouse cadaver is submitted by Laboratory Animal Production, Care, Application and Research Centre of Izmir Institute of Technology. Lungs are dissected and kept in 1 ml of ice-cold DMEM F12 (F12) containing 3-cm treated cell culture grade (TCG) Petri dishes. Experiments are carried out aseptically in Biosafety Level 2 flow cabinets (Nüve, MN 120). The Animal Care and Use Committee at Izmir Institute of Technology approves use of mice in this research.

3.3. Tissue Processing

Mechanical, enzymatic, or combined approaches are used to process lung tissues into smaller pieces.

3.3.1. Enzymatic and mechanical tissue processing

Dissected lung tissues are minced by surgical blades, collected into tubes either in 1% BSA- or 1% FBS-added, 1% penicillin/streptomycin (P/S) containing RPMI. Lung pieces are washed with either 1X PBS, 1% BSA- or 1% FBS-added 1% P/S containing RPMI. Several methods are applied to process tissues. In the first method, the centrifugate is strained through strainer. Later, lung pieces are treated with 1 ml of 1X Red Blood Cell (RBC) Lysis Buffer (Santacruz, sc-296258) for 5 minutes. Second, minced lung tissues are kept either on ice or room temperature in 1% BSA 1% P/S containing RPMI. They are centrifuged at 1000 rpm for 5 minutes and treated with 0.05% Trypsin-EDTA for 30 minutes and 0.25% Trypsin-EDTA for 1 hour. Trypsin is neutralized by 1% BSA and 1% P/S containing RPMI. Then tissues are centrifuged at 1400 rpm for 5 minutes to remove trypsin and resuspended in RPMI media. Thirdly, 1 mg ml^{-1} or 0.25 mg ml^{-1} collagenase I (from Clostridium histolyticum, Sigma-Aldrich, C9407) and 0.1 mg ml^{-1} DNase from bovine pancreas (Sigma-Aldrich, DN25) digestion mix is prepared in RPMI media. Minced lung tissues are treated with 1 mg ml^{-1} collagenase/0.1 mg ml^{-1} DNase digestion mix for 2 hours, or 0.25 mg ml^{-1} collagenase and 0.1 mg ml^{-1} DNase digestion mix for three and a half an hour. Forth, minced tissues are digested by 0.1 mg ml^{-1} collagenase/ 0.1 mg ml^{-1} DNase digestion mix, overnight. Lastly, 2 mg ml^{-1} collagenase/0.1 mg ml^{-1}

DNase digestion mix is used to process lung tissues. All enzymatic treatments are carried out on rotator at 37°C, humidified cell culture incubators with 5% CO_2. All collagenase/DNase digestion mixes are neutralized by DMEM F12 containing 100 ng.ml^{-1} cholera toxin, 0.5 ug ml^{-1} hydrocortisone, 20 ng ml^{-1} EGF, 10 ug ml^{-1} insulin, 5% DHS and 1% P/S (F12CM).

3.3.2. Mechanical tissue processing

Dissected lung tissues are roughly pieced by surgical blades and punched by biopsy puncher (Ted Pella, 15110-10) with 1 mm of outer diameter (Figure 3.2).

Figure 3.2. 1-mm biopsy punch. Ted Pella, 15110-10.

3.3.3. Optimized tissue processing protocol using needles

Dissected lung tissues are kept on ice in F12. Before starting processing, the media of tissues is changed with fresh F12. A 22G needle (Techcon, AD722, Figure 3.3) is fixed to Luer lock syringe pumps. Fresh media is drawn into the syringe before lung tissues are punched by 22G needle. The excessive fresh media in the syringe is used to pump out intact lung punches, which are collected into Eppendorf tubes in 20 ul of F12. Experiments are performed on ice. Collected punched lung tissues are used in experiments directly.

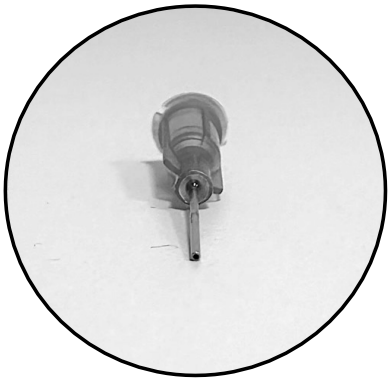

Figure 3.3. 22G needle. Outer diameter = 0.718 mm ; inner diameter = 0.413 mm.

3.4. Establishment of lung MPS

Punched lung tissues are mixed with Growth Factor Reduced Matrigel (GFR Matrigel) (Corning, 354230). For Matrigel experiments, 20 ul of 4.2 $mg.ml^{-1}$ Matrigel:tissue mix is loaded into A2 of MPS. Lung MPS is placed onto the plate adaptors upside down in 14-cm glass Petri dishes filled with 100 ml of autoclaved upH_2O to prevent Matrigel from drying. Autoclaved upH_2O does not have direct contact with MPS. Matrigel is polymerized for 30 minutes at 37°C in a humidified cell culture incubator with 5% CO_2. Later, A1 and A3 are loaded with 40 ul of F12 media (Figure 3.4).

3.5. Tissue viability

3.5.1. Fluorescence staining

Punched lung tissues are cultured in 96-well plates in 80 ul of fluorescence dye containing F12 media with different dye concentrations. Staining group of 33 ug ml^{-1} Hoechst 33258 (Sigma, 14530) and 3.3 ug ml^{-1} propidium iodine (PI, Sigma, P4170) is measured at 30, 60 and 90 minutes. 1 mg ml^{-1} Hoechst 33258 and 2 ug ml^{-1} PI- stained group is incubated overnight. 2 ug ml^{-1} calcein, AM (ThermoFisher, Scientific, C1430) and 2 ug ml^{-1} PI-stained group is measured at 15, 30, 60 and 120 minutes and overnight. Lastly, 1 ug ml^{-1} calcein AM, and 20 ug ml^{-1} Hoechst 33258 stained group is incubated for 20 minutes. The samples are measured by Leica SP8 Confocal Microscope with excitation and emission wavelengths of stains found in the manufacturer's instructions.

3.5.2. Tissue viability using alamarBlue

Tissue viability is assessed in lung MPS. The media in A1 and A3 are replaced by 40 ul of F12 containing 10% alamarBlue (ThermoFisher, Scientific, DAL1025). To assess optimal alamarBlue incubation time, lung MPS is measured by confocal microscope (Leica SP8 Confocal Microscope) every 4 hours for 24 hours starting on the day 2 of punched lung tissue cultures. AlamarBlue signal is determined by excitation at 552 nm and emission at 590 nm.

Different culture media are also tested to maximize lung tissue viability on day 3 of tissue culture. These media include 1) F12; 2) F12 containing 5% donor horse serum (F12DHS); 3) F12 supplemented with 20 $ng.ml^{-1}$ epidermal growth factor (EGF) and 10 $ug.ml^{-1}$ insulin (F12EGFINS); 4) F12CM. In all cases, punched tissues are loaded into 96-well plates with 80 ul of media in day 1. Tissue viability is determined on day 1 and day 3. The culture media is replaced by 80 ul of corresponding media containing 10% alamarBlue. The alamarBlue reduction is measured by Zeiss Axio Observer Fluorescence Microscope after 20 hours incubation.

Fluorescence images are quantified in Fiji. First, images of experimental groups are stacked. An area of interest is specified as 100x100. Mean grey values are measured on each sample. Values of all punched tissues are divided by the negative control of the experimental group, which is alamarBlue containing Matrigel- only sample for MPS experiments or alamarBlue containing media-only wells for suspension cultures. Means are plotted.

3.6. Cell culture and maintenance

MDA-MB-231 (HTB-26), a human breast cancer cell line, is obtained from ATCC. Metastatic MDA-MB-231 clones are stably labelled with a red fluorescent protein (dsRed) (Firatligil-Yıldırır & Batı-Ayaz, 2021). MDA-MB-231 cells are cultured in DMEM high glucose media containing 10% fetal bovine serum (FBS) and 1% penicillin/streptomycin (P/S), namely GM. For subculturing, the culture media is removed, and cells are briefly rinsed with 1 ml of 1X PBS. 1X PBS is replaced by 1 ml of 0.05% (w/v) Trypsin-EDTA (Trypsin C) solution. Trypsin treated cells are kept at 37°C

for 4 minutes until the cell layer is dispersed. 1 ml of GM is added to neutralize trypsin. Cells are gently pipetted and collected into tubes, which are centrifuged at 3800 rpm for 5 minutes. Supernatant is removed and cellular pellet is dissolved in 1 ml of GM. Cells are cultured with 1:4 or 1:5 cell ratio in 6-cm TCG Petri dishes. Media is renewed when required, usually within 3 days.

Human monocytic U-937 cells are gifted by Cumhur Tekin Lab at Izmir Institute of Technology. U-937 cells are stably labelled with green fluorescent protein (GFP) by Özden Yalçın Özuysal Lab at Izmir Institute of Technology. U-937 cells are cultured in GM. Because U-937 cells are monocytes, they are suspending cells. When subculture is required, all media is collected into tubes and centrifuged at 150 g for 5 minutes. Supernatant is removed and cell pellet is resuspended with fresh GM. They are seeded in fresh GM on TCG Petri dishes with subculture ratio of 1:5. Media is renewed by resuspending cells with fresh media and seeding on TCG Petri dishes directly every 3 days.

All cells are cultured at 37°C in a humidified cell culture incubator with 5% CO2. Before experiments, cells are counted by trypan blue exclusion assay.

3.7. 231CM harvest

Collection of MDA-MB-231 conditioned media (231CM) is schematically described in Figure 3.6. dsRed MDA-MB-231 cells ($2.5x10^5$ cells.ml^{-1}) are seeded in TCG 6-well plates in GM for 36 hours. GM is replaced by serum-free DMEM high glucose (DMEM SF). After 48 hours, MDA-MB-231-conditioned DMEM high glucose is collected into tubes and centrifuged at 13 300 rpm for 15 minutes. Supernatants are filtered using 0.22 um PET membrane syringe filter systems to remove cellular debris. 231CM is always freshly used.

3.8. Differentiation of U-937 cells

GFP U-937 cells are seeded in TCG 6-well plates at the concentration of $6x10^5$ cells/well. Cells are treated with 0 ng ml^{-1}, 10 ng ml^{-1}, 20 ng ml^{-1}, 50 ng ml^{-1} and 100 ng ml^{-1} concentrations of PMA in GM for 24 hours. The differentiation of GFP U-937 cells is observed with bright-field microscopy using Zeiss Axio Observer. For MPS

experiments, GFP U-937 cells are seeded at $3.33x10^5$ cells ml^{-1} in 6-cm nontreated TCG plates and cultured in GM containing 10 ng ml^{-1} PMA for 24 hours (Figure 3.6). Later, the differentiated cells are collected in Falcon tubes and centrifuged at 150 g for 5 minutes. PMA-containing GM is replaced by 231CM to use in invasion and infiltration assays.

3.9. Invasion and infiltration assays

To assess breast cancer invasiveness towards lung tissue, monoculture invasion assay is performed. To understand how invasiveness of breast cancer cells is affected by the presence immune cells, co-culture invasion and infiltration assay is modelled.

3.9.1. Monoculture invasion assay

Lung MPS is used for monoculture invasion assays (Figure 3.5). For tissue-free condition (control), Matrigel is diluted with ice-cold F12 to a final concentration of 4.2 mg ml^{-1} and loaded into A2. To assess invasiveness towards punched tissues, a single punched lung is mixed with Matrigel to final concentration of 4.2 mg ml^{-1} and loaded A2. Matrigel is polymerized as given in Title 3.4. Later, dsRed MDA-MB-231 cells ($1x10^6$ cells ml^{-1}) are loaded into A1 of control and lung condition in F12. A3 is filled with F12 media. Lung MPS' are incubated for 72 hours. The invasion of dsRed MDA-MB-231 cells is first imaged after 2 hours by confocal microscope. Lung MPS' are imaged every 24 hours for 3 days.

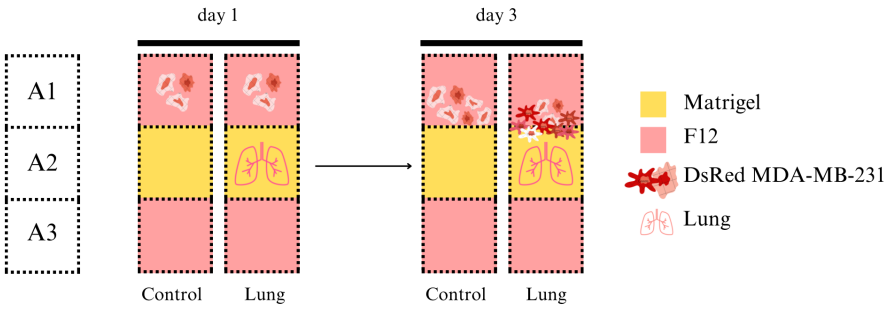

Figure 3.4. Monoculture invasion assays. Matrigel:punched lung tissue is loaded into A2. DsRed MDA-MB-231 cells and F12 is added to A1 and A3, respectively. Chips are imaged after 2 hours and every 24 hours for 3 days.

3.9.2. Co-culture invasion and infiltration assay

To understand breast cancer invasiveness towards punched lung tissues in the presence of immune cells, co-culture invasion and infiltration assay is performed (Figure 3.6). Immune cells are modelled by PMA-differentiated GFP U-937 cells. For co-culture experiments, 231CM and differentiated GFP U-937 cells are readily prepared. For all conditions, Matrigel is diluted to 4.2 mg ml^{-1} with F12 and polymerized. Later A1 is loaded by i) $5x10^5$ cells ml^{-1} dsRed MDA-MB-231 cells in 231CM ii) $1.66x10^5$ cells ml^{-1} GFP U-937 cells in 231CM, iii) $5x10^5$ cells ml^{-1} dsRed MDA-MB- 231 cells and $1.66x10^5$ cells ml^{-1} GFP U-937 cells in 231CM as co-culture. A3 is filled with F12 media. After 24 hours, a single punched tissue is placed into A3 of each condition. As control experiment, media in A3 is renewed.

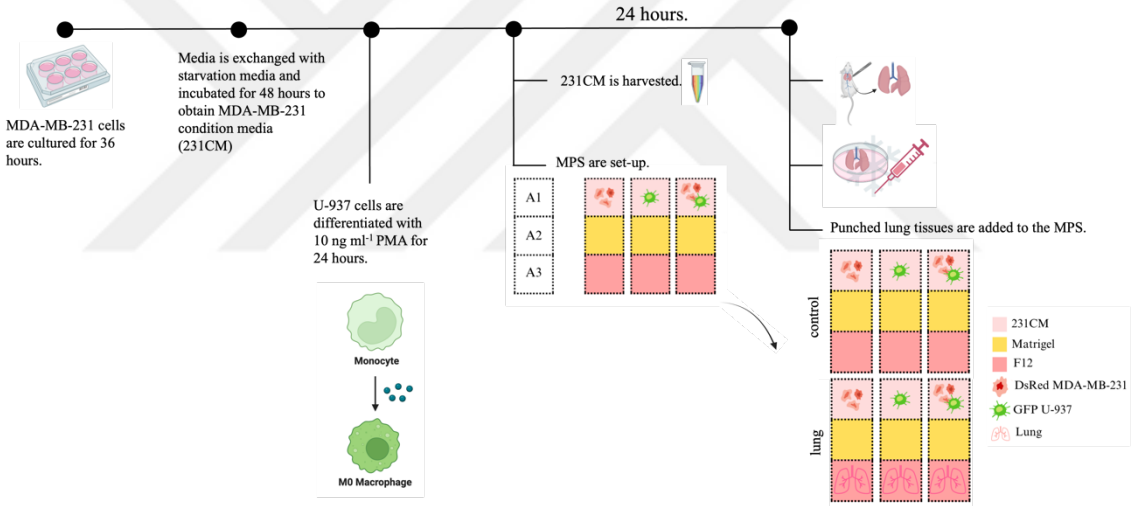

Figure 3.5. Illustration of invasion and infiltration assay. 231CM is harvested and used freshly. GFP U-937 cells are differentiated with 10 $ng.ml^{-1}$ PMA. Matrigel is loaded into A2. MDA-MB-231 cells, U-937 cells or co-culture of the two cell lines are added in 231CM to A1. A3 is loaded with F12. Punched lung tissues are put into the system 24 hours. Chips are imaged every 24 hours for 3 days.

3.9.3. Quantification of invasion and infiltration assays

Z-stack images are acquired on confocal microscope with following parameters: a 10X objective and a z-step size of 7.52 um. The sum projection of z-stacks is processed in Fiji. Threshold images are acquired and the distance from start line to individual bright pixels are recorded by Python programming (Figure 3.7). The migration of cells is calculated in R Studio through normalization of all data to the first day datasets as previously explained (Ilhan et al., 2020).

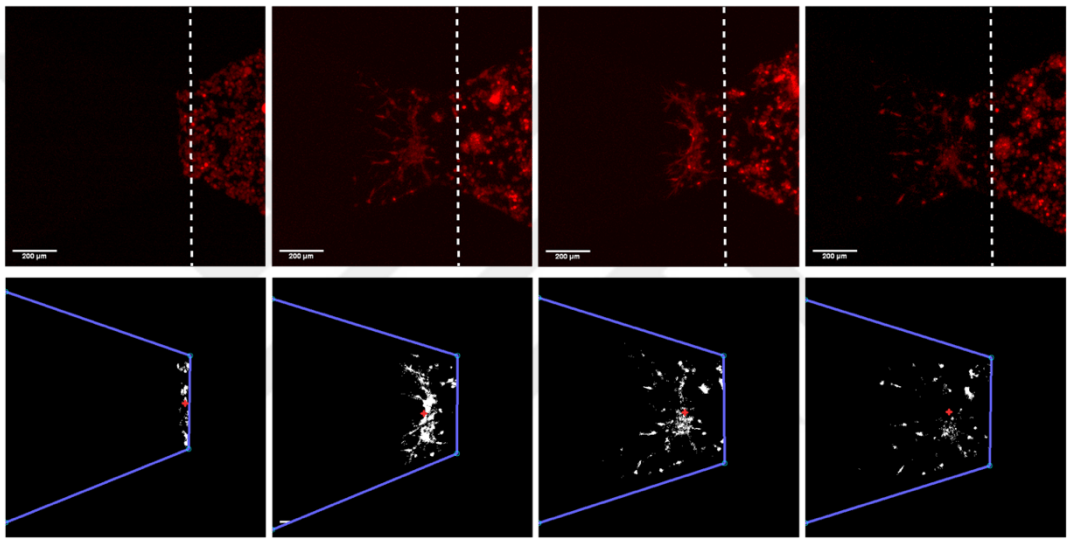

Figure 3.6. An example image processing from Z-sum projection to threshold using Python programming. a) Z-sum projection of dsRed MDA-MB-231 cells. b) Threshold images. Red dots represent the centre of gravity of all bright pixels. Python measures the distance of each bright pixel from the starting line. Scale bar = 200 um.

3.10. Statistical analysis

For all experimental groups of viability, invasion, and infiltration assays, at least 3 experiments are analysed. The number of biological replicates is given as “n” in the figure legends. Replicates that fail outlier analysis using percentile are removed. Results are reported as mean ± SEM. Student’s t-test is applied and a p-value <.05 is determined as significant.

CHAPTER 4

RESULTS

4.1. Biopsy punches preserve tissue integrity and provide consistent size distribution.

Mechanical, enzymatic, or combined approaches are used to process tissues in literature. One of the first aims of this study is to develop a tissue processing method that protects tissue integrity to a degree. In Figure 4.1, used enzymatic approaches and respective results are given. After mincing by surgical blades, trypsinization and collagenase/DNase digestion mixes generally resulted in unequal tissue pieces with stromal cells. Even with well washing steps, tissues were broken down to single cells. Trypsin is an enzyme that digest adhering proteins of cells. Collagen is one of the main proteins in lung microenvironment (Hackett et al, 2022). Therefore, using proteases such as trypsin and collagenase disrupted tissue integrity inconsistently. In addition, one unfortunate occurrence during washings, lung pieces were floating despite of centrifugation steps which was causing sample loss. Overall, enzymatic, and mechanical approach did not provide an alternative for tissue processing in terms of goals in this study.

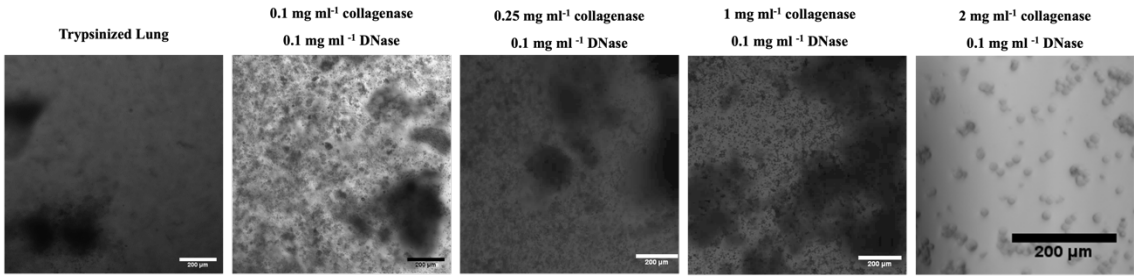

Figure 4.1. Enzymatic processes after dissected lung tissues are minced by blades. Digestive enzymes are given above images. In all samples tissue architecture is disrupted heavily, yielding uneven tissue pieces as well as single cls. Scale bar = 200 um.

With the aim of preserving tissue architecture and extracellular matrix components with stromal cells, tissues are processed by 1 mm-biopsy punches (Figure 3.2). Punches generated even tissue pieces around 400 um in diameter (Figure 4.2). These punched lung tissues were round, seemingly preserving tissue integrity. There were not stromal cells around tissue pieces; hence, the system was promising.

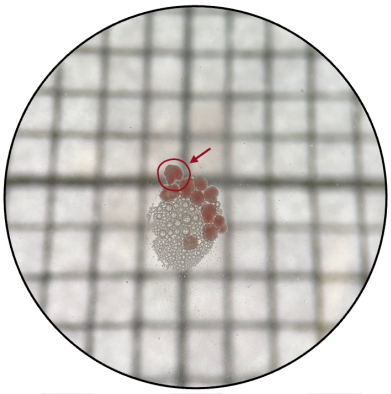

Figure 4.2. Punched lung tissues using 1-mm biopsy punch. A single tissue is encircled on millimetric paper. Imaged using stereomicroscope.

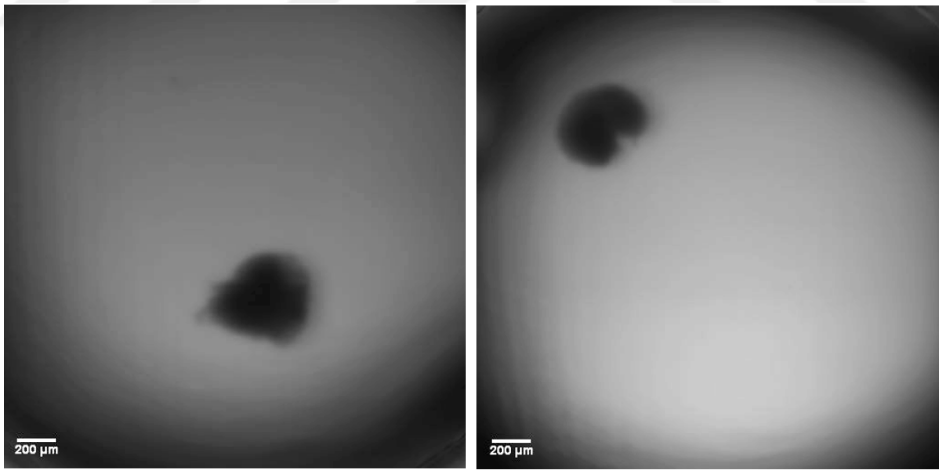

Figure 4.3. Punched lung tissues using 22G needle. Observed in bright-field microscopy, 10x. Scale bar = 200 um

Furthermore, a 22G needle with inner diameter of 0.413 mm was used to replace 1-mm biopsy punches (Figure 3.3). Because 22G needles could be autoclaved and reusable, the cost of the tissue processing technique is decreased significantly compared

to sophisticated equipment such as vibratome. Using a syringe with 22G needle yielded perfectly round tiny, punched lung tissues with 300-400 um diameter (see Figure 4.3). These tissues preserve their extracellular matrix. Stromal cells did not disperse. Tissue pieces were easily pipetted using 200-ul micropipette tips. In conclusion, 22G needle is found to be the most convenient tool to process lung tissues into smaller punched lung tissues to conserve tissue integrity.

4.2. Lung tissues retain viable up to 72 hours.

All tissue processing techniques are damaging and can affect cellular viability within the tissues. Thus, using fluorescence stains or metabolic assays, tissue viability should be determined for prolonged culture conditions. First, Hoechst 33258/PI staining is applied. Hoechst 33258 is a cell permeable dye that can bind to DNA. Therefore, it stains all cells whereas PI is cell impermeable and can detect dead cells. Unfortunately, the residual stains caused background signal for both reagents making impossible to detect tissue viability in enzymatic digestion methods (Figure 4.4.a). The same situation was seen in Blue/Green Live/Dead assay as well (Figure 4.4.b).

On the other hand, enzymatic processes were eliminated in experimental setups and punches were decided to be used. Thus, calcein AM/PI staining is applied to punched lung tissues from 1-mm biopsy punch. Calcein AM is metabolized by living cells and cannot leave the cells once esterified. Therefore, using Calcein AM with PI was expected to distinguish between living and death cells of punched lung tissues (Figure 4.4.c). However, it was not possible to determine the degree of viability because PI signal was causing background noise. Later, PI is replaced by Hoechst 33258 (Figure 4.4.d); but eventually fluorescence staining was decided to be complicated to quantify and/or analyse viability.

Next, to assess cellular viability, a metabolic cell viability reagent called alamarBlue (ThermoFisher Scientific, DAL1025) is used. AlamarBlue is a blue solution, which includes resazurin. When it diffuses into living cells, resazurin is reduced to resorufin and solution colour changes to pink. AlamarBlue can also be detected fluorescently. In order to use alamarBlue to check tissue viability, first; required incubation time is decided. In manufacturer's instructions, alamarBlue is incubated for 4 hours to determine cellular viability. Yet, tissues are larger pieces and consists of

extracellular environment that can affect the diffusion of reagent. Therefore, punched samples are imaged every 4 hours for 24 hours to detect optimal time of incubation (Figure 4.5.a). Ultimately, 20 hours incubation is decided to be best. Later, the suitable media are tested to maximize tissue viability. Punched lung tissues are suspended in F12 media, F12DHS media, F12EGFINS and F12CM. AlamarBlue reduction is measured on day 1 and 3 of lung tissue dissection (Figure 4.5.b). There was no significant difference among media samples or days; therefore, the simplest media F12 is used. Because any media supplement can also affect invasion and infiltration assays, using F12 was more convenient.

Finally, tissue viability is determined on day 3 with a larger sample size. Punched tissues are shown to retain tissue viability up to 72 hours of incubation in F12 (Figure 4.6). Tissue viability beyond this time point has not determined during these studies. In conclusion, alamarBlue reagent was determined to most convenient detection method for tissue viability in this study.

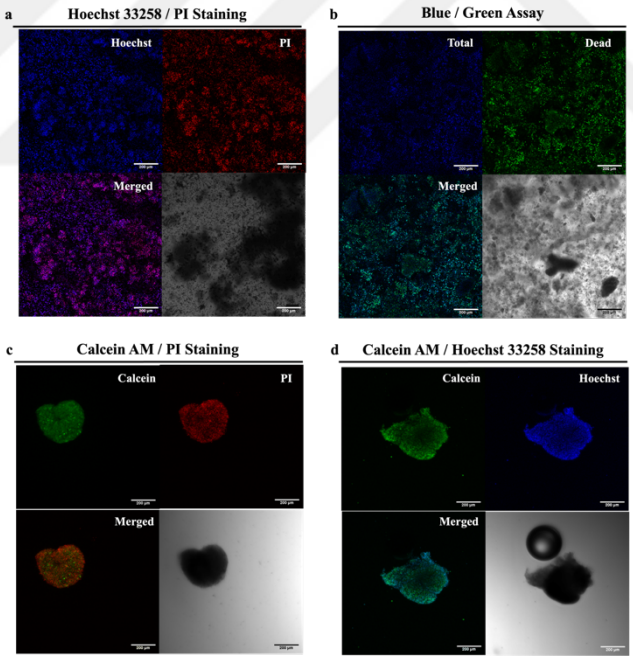

Figure 4.4. Fluorescence staining of tissue samples. a, b) Tissues after collagenase/DNase digestion mixture. a) Staining of tissue pieces using Hoechst 33258 and PI. b) Staining of tissue remaining with Blue/Green Live/Death assay. c) Staining of punched lungs by calcein AM and PI. d) Staining of punched lung by calcein AM and Hoechst 33258. Images taken by Leica SP8 Confocal Microscope, 10x. Scale bar = 200 um.

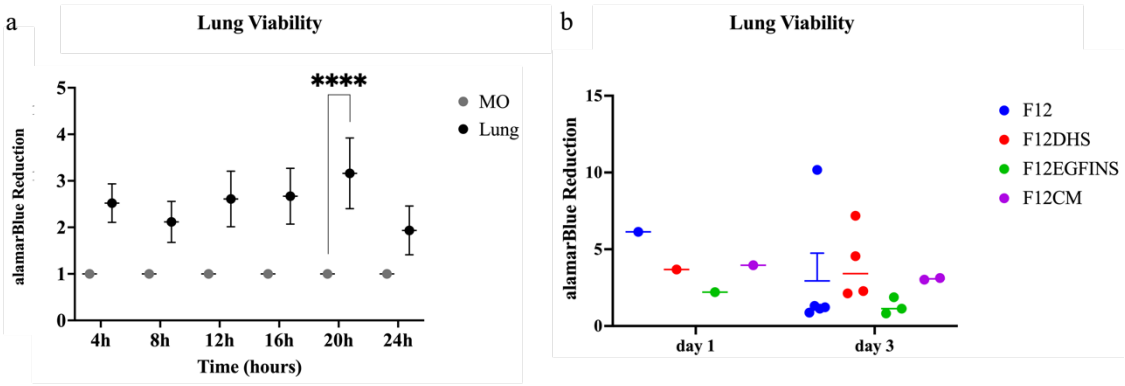

Figure 4.5. Tissue viability using alamarBlue. a) alamarBlue reduction signal is maximized at 20th hours. Student t-test is used to determine significance < .05. n = 7. b) Punched lung tissues are suspended in following media containing: 1) F12; 2) F12 containing 5% donor horse serum (F12DHS); 3) F12 supplemented with 20 ng/ml EGF epidermal growth factor (EGF) and 10 ug/ml insulin (F12EGFINS); 4) F12CM. On the day of measurement 10% alamarBlue is added to samples and signal is measured at 20th hour in Zeiss Axio Observer, 10x.

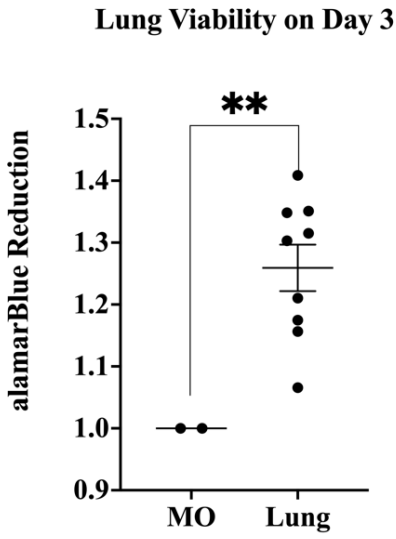

Figure 4.6. Tissue viability at 72 hours using alamarBlue. alamarBlue reduction is measured o day 3 of tissue culture in F12 using Zeiss Axio Observer. Student t-test is applied to determine significance <.05, n = 8.

4.3. MDA-MB-231 cells invade punched lung tissues.

Invasion of breast cancer cells are previously shown using organ-on-chips by Fıratlıgil-Yıldırır & Batı-Ayaz et al (2021). They showed that secreted factors from homing cells are crucial to direct dsRed MDA-MB-231 cells to invasion. In this research, lung MPS is used to show breast cancer cell migration to punched lung tissues (Figure 4.7). This result showed that lung tissue was a homing target for breast cancer cells. Because punched lung tissues are whole tissue pieces, they retain extracellular matrix and stromal cells within their structure. Because punched lung tissues are whole tissue pieces, they retain extracellular matrix and stromal cells within their structure. Therefore, they represent *in vivo* conditions better and is a promising model for lung-related metastatic research.

4.4. MDA-MB-231 cells invade punched lung tissue more in the presence of differentiated U-937 cells.

TAMs are recognized as an essential part of the tumour microenvironment. Their role in tumour metastasis has been studied extensively. At later stages of tumour progression, TAMs secrete soluble factors and proteases to remodel extracellular matrix (Huang et al, 2022). To assess the effects of macrophages in invasiveness of breast cancer cells, GFP U-937 cells were differentiated using several concentrations of PMA (10 ng ml^{-1}, 20 ng ml^{-1}, 50 ng ml^{-1} and 100 ng ml^{-1}). After treatment, monocytic cells were small and round whereas differentiated GFP U-937 cells showed macrophage-like phenotype in morphology and increased surface adherence (Figure 4.8). For all PMA-concentrations, differentiation of GFP U-937 was successful. Thus, 10 ng ml^{-1} is subsequently used. Next, differentiated GFP U-937 cells were passaged using 0.25% (w/v) Trypsin-EDTA. However, prolonged incubation after removal of PMA from media caused cells to be resuspended in treated TCG dishes suggesting GFP U-937 cells were de-differentiating. Which is why, differentiated cells should be used immediately. Macrophage-like cells were also not dispersed easily using 0.25% (w/v) Trypsin-EDTA solution; therefore, differentiation was carried out in non-treated Petri dishes to prevent loss of cells during experiment. In non-treated Petri dishes, monocytic GFP U-937 cells were small and suspended individually whereas PMA-differentiated GFP U- 937 cells

formed large homoaggregates showing another consequence of PMA-treatment. In conclusion, GFP U-937 cells are differentiated with 10 ng ml^{-1} PMA in nontreated Petri dishes for 24 hours and used immediately in lung MPS.

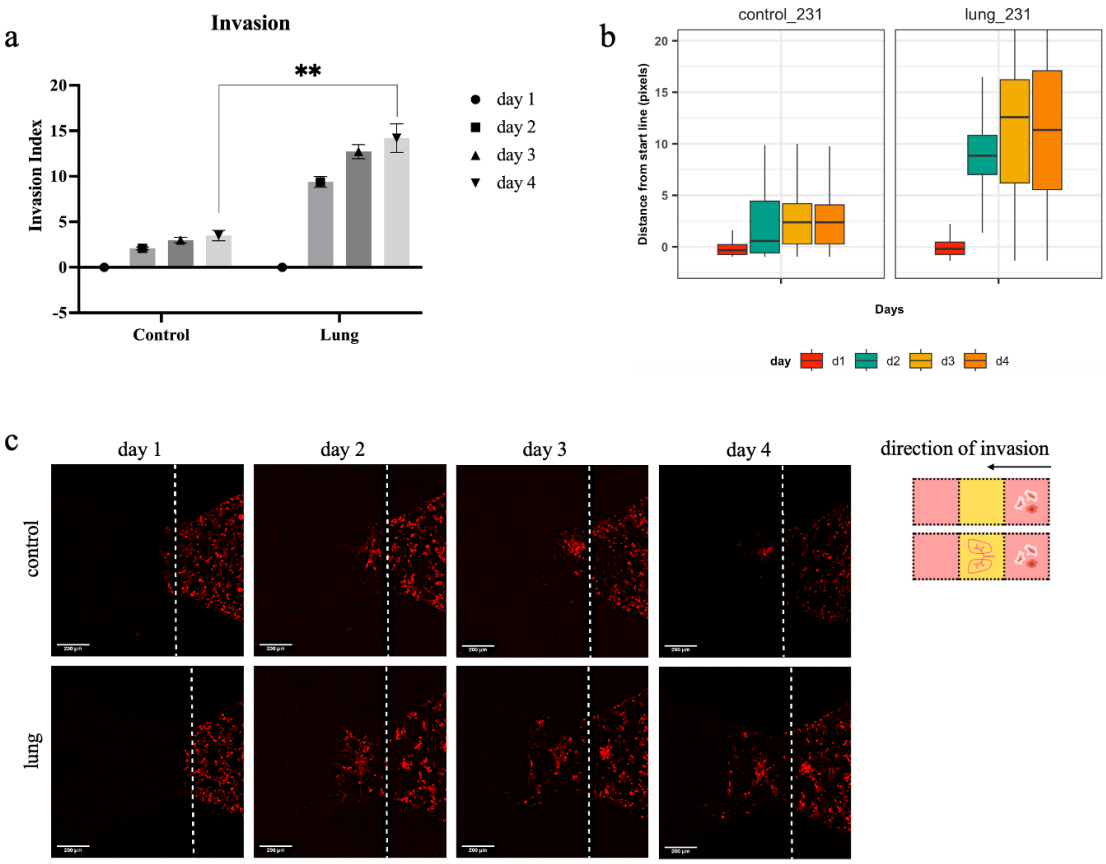

Figure 4.7. Invasion of metastatic breast cancer cells into punched lung tissues. a) The distance of dsRed MDA-MB-231 cells from starting line (dashed line) is calculated after thresholding. The data is normalized to d1 (n = 3). b) Means of normalized distances of MDA-MB-231 cells to detect invasion index on each day. c) Representative Z-stack images of control and lung condition showing migration of MDA-MB-231 cells. Dash line indicates the starting line on day 1. All results are normalized to day 1 dataset.

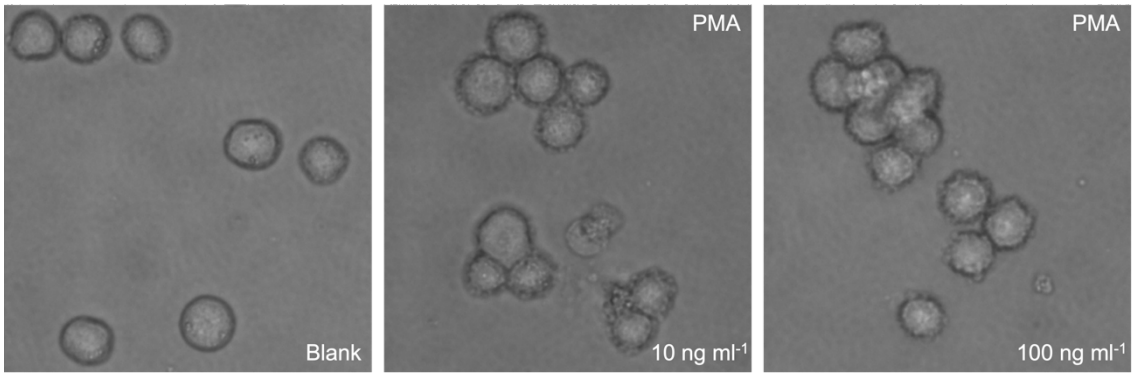

Figure 4.8. Bright-field images of GFP U-937 cells after PMA differentiation. Nontreated GFP U-937 cells are round and in suspension (left). 10 ng ml^{-1} (middle) and 100 ng ml^{-1} (right) PMA-treated GFP U-937 cells are adhered and formed homoaggregates. Zeiss Axio Observer Fluorescence Microcope, 40x.

During cell culture, MDA-MB-231 cells secrete paracrine molecules, exosomes, and soluble factors to cause inflammation; therefore, it is utilized in co-culture invasion and infiltration assay to activate PMA-treated macrophages. Before loading into MPS, PMA-differentiated GFP U-937 cells were suspended in 231CM to cause possible polarization of PMA-differentiated GFP U-937 cells (Saraiva et al, 2020).

The addition of macrophage-like cells increases invasion significantly compared to monoculture of breast cancer cells in the presence of punched lung tissue (Figure 4.9 and Figure 4.10). In addition, a significant difference between control co-culture and lung co-culture groups are seen suggesting punched lung tissue is the attractant factor for breast cancer cells in the system. Surprisingly, when monoculture conditions of this assay is compared, the difference in invasion was not significant. However, dsRed MDA-MB-231 cells are shown to metastasize to lung in Figure 4.7. This finding shows that 231CM may not be a suitable media for dsRed MDA- MB-231 cells migration since cellular waste is also accumulated. Additionally, 231CM does not support viability for prolonged culture conditions as most of cell signal is decreased in day 3 of experiment in all conditions. Further, in the absence of punched lung tissue, a decrease in invasion is seen; yet breast cancer cells and macrophages form heteroaggregates , suggesting the presence of lung could be dominating factor for invasion that is assisted by the inflammatory cells.

To understand whether PMA-differentiated and 231CM activated GFP U-937 cells infiltrate into Matrigel in any specific conditions, the migration of macrophage-like

cells is also imaged. When invasion (Figure 4.9A) and infiltration indeces (Figure 4.11A) are compared, it is seen that immune cells did not migrate much through the gel towards lung compared to breast cancer cells. It is also seen from the graphs that overtime, migrated U-937 cells regressed (Figure 4.11). This could be because of two reasons. First, U-937 cells form homoaggregates; thus, cells could be drawn back. Second, migrated cells can lose viability, which can also explain why signal is decreased on day 3 (Figure 4.10. In general, because no data was significant, infiltration of macrophages cannot be determined in this experimental setup.

Overall, in co-culture invasion and infiltration assays, GFP U-937 cells are differentiated and activated by 231CM acting as TAMs, which in return increased invasion of dsRed MDA-MB-231 cells towards punched lung tissues.

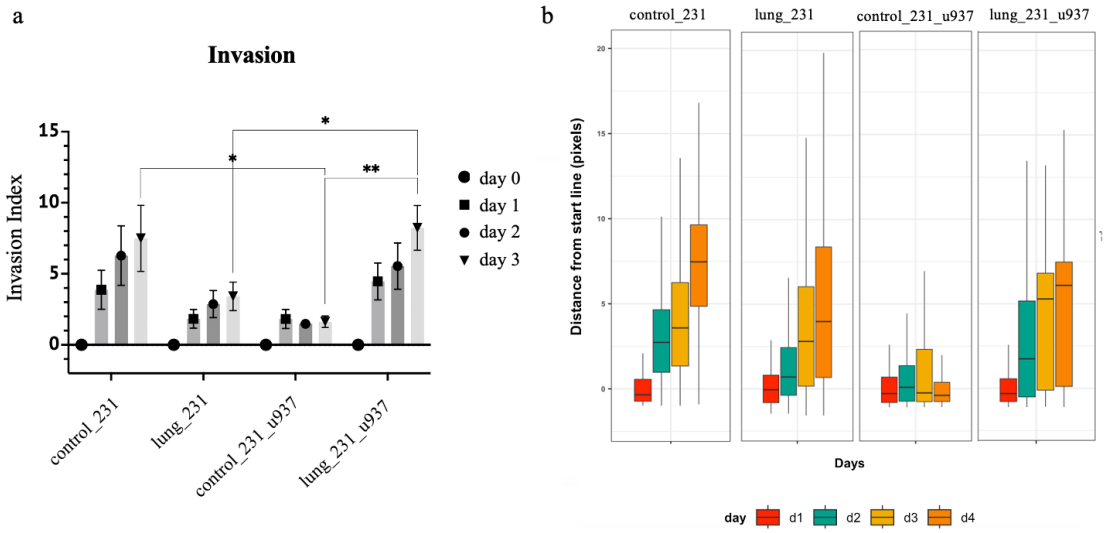

Figure 4.9. Invasion of breast cancer cells when co-cultured with macrophage-like cells in the presence and absence of punched lung tissues. (a) Mean values of normalized distances after outlier analysis. Error bars represent mean±SEM. b) Distribution of migration distances normalized to day 0 shown as box plots. n = 3.

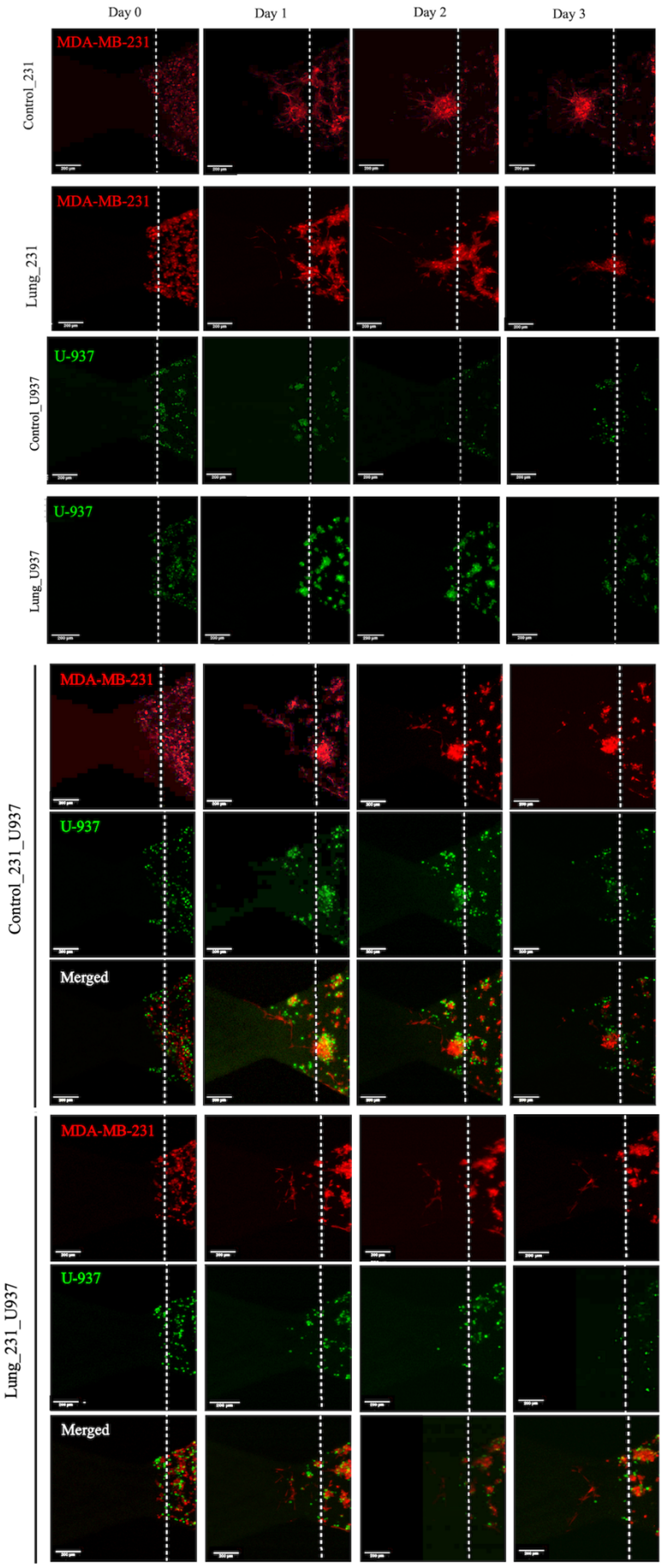
Day 0
Day 1
Day 2
Day 3
Control_231
MDA-MB-231
Lung_231
MDA-MB-231
Control_U937
U-937
Lung_U937
U-937
Control_231_U937
MDA-MB-231
U-937
Merged
Lung_231_U937
MDA-MB-231
U-937
Merged

Figure 4.10. Representative Z-sum projections of co-culture invasion and infiltration assays. Images shows the migration/invasion/chemotaxis of MDA-MB-231 and U-937 cells to punched lung tissues. Dashed lines are accepted as starting axes, scale bar = 200 um.

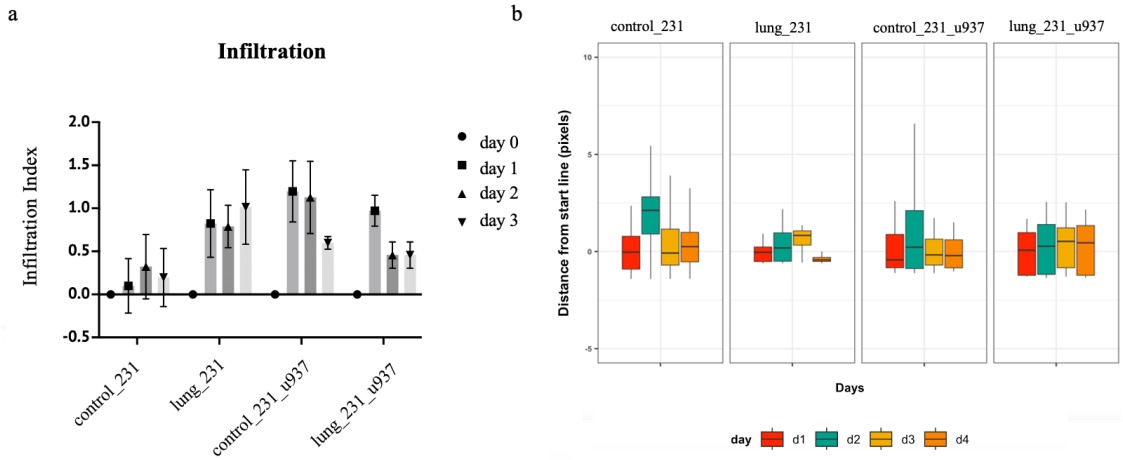

Figure 4.11. Infiltration of macrophage-like cells when co-cultured with breast cancer cells. (a) Mean values of normalized distances is plotted after outlier analysis. Error bars represent mean ± SEM. (b) distribution of migration distances normalized to day 0 shown as box plots. n = 3.

CHAPTER 5

DISCUSSION

Metastasis is a major driver of breast cancer-related mortality, and lung metastasis is one of the most common patterns of spread. The study of breast cancer metastasis to the lung provides valuable insights into the biology of cancer progression. Because 3D lung models offer better replicate the 3D structure and microenvironment of the lung tissue, a comprehensive model is a valuable tool to study factors that govern metastatic processes, which can contribute to the advancement of personalized medicine. Therefore, it was aimed to develop a tissue-based 3D lung model that preserves tissue integrity to study breast cancer metastasis. The platform is also used to study effects of macrophages during cellular invasion of breast cancer cells.

In this study, a novel tissue processing technique known as the biopsy punch, employing 22G needles as its primary tool has been introduced. The choice of a 22G needle for this purpose is notable for its accessibility and cost-effectiveness, making it a practical alternative to more expensive methods such as microtomes and vibratomes. The affordability of 22G needles, readily available in many laboratory settings, presents a significant advantage in reducing overall research costs. One of the key findings of this technique is its ability to maintain the viability of punched lung tissues for up to 72 hours following lung dissection and processing in DMEM F12 with 1% penicillin/streptomycin supplementation. This extended viability is crucial for various experimental purposes, allowing researchers a more extensive window of opportunity for conducting experiments and analyses. Furthermore, the use of a defined culture medium, DMEM F12, offers precise control over the lung microenvironment, a feature that distinguishes this technique from other lung tissue cultures involving precision-cut lung slices (Sun et al, 2023). Notably, the biopsy punch technique does not employ any media media or gel to fill the lungs to avoid disrupting lung structure during processing, which is a step required during sectioning (Sun et al., 2023; Alsafadi et al., 2020) and culturing (Bailey et al., 2020). This streamlined approach simplifies tissue processing and reduces potential sources of experimental variability that may arise from variations in media or gel composition. In conclusion, the introduction of the biopsy punch technique using 22G needles represents a significant advancement in tissue processing for lung-related studies. Its cost-

effectiveness, extended tissue viability, and avoidance of complex media or gel requirements make it a valuable tool in experimental settings. This innovative approach not only enhances the efficiency of lung tissue research but also offers more precise and cost-efficient investigations in the field many pulmonary-related diseases including lung metastasis.

Lungs are a frequent site for metastasis in triple-negative breast cancer (TNBC), accounting for 40% of such cases as reported by Wang et al. (2022), underscores the clinical significance of investigating metastatic processes within this organ. In the present study, we have taken a significant step in using biopsy punch method to obtain punched lung tissues, which then cultured in 3D microphysiological system to study breast cancer metastasis. The use of intact lung tissues for the investigation of breast cancer cell invasion distinguishes our research from previous studies and constitutes a critical advancement in the field. While various methods have been employed to study metastasis, including the use of cell lines, animal models, and *ex vivo* precision cut lung slices, none have exclusively utilized intact lung tissues for this purpose. As a result, our study represents a pioneering effort in providing a more physiologically relevant and holistic model for investigating breast cancer metastasis to the lungs.

The interaction between breast cancer cells and macrophage-like cells within the context of metastasis to the lungs is a complex and dynamic process. It is well-established that macrophages play a crucial role in the tumour microenvironment, with the potential to influence cancer progression in various ways. In this research, an increase in breast cancer cell metastasis to the lung is observed in the presence of macrophage-like cells, consistent with findings by Song et al. (2019), who reported that MDA-MB-231 aggregates activated monocytes (U-937) to adopt a tumour-associated macrophage (TAM)-like phenotype. Furthermore, the promotion of breast cancer cell invasion, migration, and proliferation by M2-like tumour-associated macrophages aligns with the research by Chen et al. (2022). Their work suggests a potential mechanism involving the epithelial-mesenchymal transition (EMT). This finding underscores the complexity of the interplay between cancer cells and immune cells and suggests that EMT may be a key mediator of enhanced metastatic potential in the presence of certain immune cell subtypes. This interaction between cancer cells and macrophage-like cells appears to be multifaceted, involving intricate signalling mechanisms. While our study provides valuable insights into the impact of macrophage-like cells on breast cancer cell metastasis to the lung, it is important to acknowledge that our experiments did not conclusively

establish the infiltration of tumour-associated immune cells into lung tissue. Future studies should aim to address this aspect in a more comprehensive manner. Another parameter that is important in the study of cancer cell invasion and infiltration is the role of endothelial cells. The presence of endothelial cells, which constitute the inner lining of blood vessels, can significantly impact the migration of cancer cells and immune cells across vascular barriers. Including endothelial cells in our experimental setup could provide a more accurate representation of the dynamic interactions that occur during cancer cell metastasis to the lung. This addition may shed light on the intricate interplay between cancer cells, immune cells, and the vascular system, offering a more holistic understanding of the metastatic process.

In conclusion, this study offers a robust 3D tissue model in which critical aspects of breast cancer metastasis to lung can be studied. This method pioneers the utilization of intact lung tissues as a substrate for breast cancer cell invasion, setting it apart from previous research relying on cell lines, animal models, or precision-cut lung slices. This approach offers a more physiologically relevant and holistic model for studying breast cancer metastasis to the lungs which is a cost-effective and accessible alternative. The research promises future directions, including the screening of antimetastatic drugs, exploration of underlying molecular mechanisms for novel drug target identification, extension of the model to study metastasis in other organs, and its application to various types of adenocarcinomas. In summary, this study presents a comprehensive exploration of breast cancer metastasis to the lung, introducing innovative techniques and models that have the potential to advance our understanding of this complex process. By optimizing tissue processing, 3D cell culture, and invasion/infiltration platforms, this research provides valuable tools for metastasis research and opens exciting avenues for future investigations in the field of cancer biology and therapy.

REFERENCES

Alsafadi, H. N., Uhl, F. E., Pineda, R. H., Bailey, K. E., Rojas, M., Wagner, D. E., & Königshoff, M. 2020. "Applications and approaches for three-dimensional precision-cut lung slices. disease modeling and drug discovery." *American Journal of Respiratory Cell and Molecular Biology*, *62*(6), 681–691. https://doi.org/10.1165/rcmb.2019-0276tr

Alzeeb, G., Metges, J.-P., Corcos, L., & Le Jossic-Corcos, C. 2020. "Three-dimensional culture systems in Gastric Cancer Research." *Cancers*, *12*(10), 2800. https://doi.org/10.3390/cancers12102800

Bailey, K. E., Pino, C., Lennon, M. L., Lyons, A., Jacot, J. G., Lammers, S. R., Königshoff, M., & Magin, C. M. 2020. "Embedding of precision-cut lung slices in engineered hydrogel biomaterials supports extended *ex vivo* culture." *American Journal of Respiratory Cell and Molecular Biology*, *62*(1), 14–22. https://doi.org/10.1165/rcmb.2019-0232ma

Chen, Z., Wu, J., Wang, L., Zhao, H., & He, J. 2022. "Tumor-associated macrophages of the M1/M2 phenotype are involved in the regulation of malignant biological behavior of breast cancer cells through the EMT pathway." *Medical Oncology*, *39*(7). https://doi.org/10.1007/s12032-022-01670-7

Firatligil-Yildirir, B., Bati-Ayaz, G., Tahmaz, I., Bilgen, M., Pesen-Okvur, D., & Yalcin-Ozuysal, O. 2021. "On-chip determination of tissue-specific metastatic potential of breast cancer cells." *Biotechnology and Bioengineering*, *118*(10), 3799–3810. https://doi.org/10.1002/bit.27855

Habanjar, O., Diab-Assaf, M., Caldefie-Chezet, F., & Delort, L. 2021. "3D cell culture systems: Tumor application, advantages, and disadvantages." *International Journal of Molecular Sciences*, *22*(22), 12200. https://doi.org/10.3390/ijms222212200

Hackett, T.-L., Vriesde, N. R., AL-Fouadi, M., Mostaco-Guidolin, L., Maftoun, D., Hsieh, A., Coxson, N., Usman, K., Sin, D. D., Booth, S., & Osei, E. T. 2022. "The role of the dynamic lung extracellular matrix environment on fibroblast

morphology and inflammation." *Cells*, *11*(2), 185. https://doi.org/10.3390/cells11020185

Hoarau-Véchot, J., Rafii, A., Touboul, C., & Pasquier, J. 2018. "Halfway between 2D and animal models: Are 3D cultures the ideal tool to study cancer-microenvironment interactions?" *International Journal of Molecular Sciences*, *19*(1), 181. https://doi.org/10.3390/ijms19010181

Huang, X., Cao, J., & Zu, X. 2021. "Tumor-associated macrophages: An important player in breast cancer progression." *Thoracic Cancer*, *13*(3), 269–276. https://doi.org/10.1111/1759-7714.14268

Humbert, M. V., Spalluto, C. M., Bell, J., Blume, C., Conforti, F., Davies, E. R., Dean, L. S. N., Elkington, P., Haitchi, H. M., Jackson, C., Jones, M. G., Loxham, M., Lucas, J. S., Morgan, H., Polak, M., Staples, K. J., Swindle, E. J., Tezera, L., Watson, A., & Wilkinson, T. M. A. 2022. "Towards an artificial human lung: Modelling organ-like complexity to aid mechanistic understanding." *European Respiratory Journal*, *60*(6), 2200455. https://doi.org/10.1183/13993003.00455-2022

Ilhan, M., Kucukkose, C., Efe, E., Gunyuz, Z. E., Firatligil, B., Dogan, H., Ozuysal, M., & Yalcin-Ozuysal, O. 2020. "Pro-metastatic functions of Notch signaling is mediated by cyr61 in breast cells." *European Journal of Cell Biology*, *99*(2–3), 151070. https://doi.org/10.1016/j.ejcb.2020.151070

Jensen, C., & Teng, Y. 2020. "Is it time to start transitioning from 2D to 3D cell culture?" *Frontiers in Molecular Biosciences*, *7*. https://doi.org/10.3389/fmolb.2020.00033

Knutsdottir, H., Condeelis, J. S., & Palsson, E. 2016. "3-D individual cell based computational modeling of tumor cell–macrophage paracrine signaling mediated by EGF and CSF-1 gradients." *Integrative Biology*, *8*(1), 104–119. https://doi.org/10.1039/c5ib00201j

Medeiros, B., & Allan, A. L. 2019. “Molecular mechanisms of breast cancer metastasis to the lung: Clinical and experimental perspectives.” *International Journal of Molecular Sciences*, *20*(9), 2272. https://doi.org/10.3390/ijms20092272

Nascimento, C. R., Rodrigues Fernandes, N. A., Gonzalez Maldonado, L. A., & Rossa Junior, C. 2022. “Comparison of monocytic cell lines U937 and THP-1 as macrophage models for in vitro studies.” *Biochemistry and Biophysics Reports*, *32*, 101383. https://doi.org/10.1016/j.bbrep.2022.101383

Pan, Y., Yu, Y., Wang, X., & Zhang, T. 2020. “Tumor-associated macrophages in tumor immunity.” *Frontiers in Immunology*, *11*. https://doi.org/10.3389/fimmu.2020.583084

Saraiva, D. P., Matias, A. T., Braga, S., Jacinto, A., & Cabral, M. G. 2020. “Establishment of a 3D co-culture with MDA-MB-231 breast cancer cell line and patient-derived immune cells for application in the development of immunotherapies.” *Frontiers in Oncology*, *10*. https://doi.org/10.3389/fonc.2020.01543

Shah, D. D., Raghani, N. R., Chorawala, M. R., Singh, S., & Prajapati, B. G. 2023. “Harnessing three-dimensional (3D) cell culture models for pulmonary infections: State of the art and Future Directions.” *Naunyn-Schmiedeberg’s Archives of Pharmacology*. https://doi.org/10.1007/s00210-023-02541-2

Song, C., Gao, D., Yuan, T., Chen, Y., Liu, L., Chen, X., & Jiang, Y. 2019. “Microfluidic three-dimensional biomimetic tumor model for studying breast cancer cell migration and invasion in the presence of interstitial flow.” *Chinese Chemical Letters*, *30*(5), 1038–1042. https://doi.org/10.1016/j.cclet.2019.02.017

Sun, Y., Jing, P., Gan, H., Wang, X., Zhu, X., Fan, J., Li, H., Zhang, Z., Lin, J. C., & Gu, Z. 2023. “Evaluation of an ex vivo fibrogenesis model using human lung slices prepared from small tissues.” *European Journal of Medical Research*, *28*(1). https://doi.org/10.1186/s40001-023-01104-8

Vanderburgh, J., Sterling, J. A., & Guelcher, S. A. 2016. “3D printing of tissue engineered constructs for in vitro modeling of disease progression and drug screening.” *Annals*

of Biomedical Engineering, *45*(1), 164–179. https://doi.org/10.1007/s10439-016-1640-4

Wang, J., Zhao, H., Ye, L., Li, J., Zhang, H., Zhang, C., Rao, Q., Cai, Y., Xu, Y., & Deng, Y. 2022. "Diagnostic and prognostic nomograms for lung metastasis in triple-negative breast cancer." *Computational and Mathematical Methods in Medicine*, *2022*, 1–12. https://doi.org/10.1155/2022/1750834

World Health Organization. n.d. "*Breast cancer*." World Health Organization. https://www.who.int/news-room/fact-sheets/detail/breast-cancer

Wu, Q., Li, J., Zhu, S., Wu, J., Chen, C., Liu, Q., Wei, W., Zhang, Y., & Sun, S. 2017. "Breast cancer subtypes predict the preferential site of distant metastases: A seer based study." *Oncotarget*, *8*(17), 27990–27996. https://doi.org/10.18632/oncotarget.15856

Wu, Z., & Lu, J. 2018. "Advances in treatment of metastatic breast cancer with bone metastasis." *Chinese Clinical Oncology*, *7*(3), 31–31. https://doi.org/10.21037/cco.2018.06.05

Yousefi, M., Nosrati, R., Salmaninejad, A., Dehghani, S., Shahryari, A., & Saberi, A. 2018. "Organ-specific metastasis of breast cancer: Molecular and cellular mechanisms underlying lung metastasis." *Cellular Oncology*, *41*(2), 123–140. https://doi.org/10.1007/s13402-018-0376-6